A Novel Eco-Friendly Vanadium Precipitation Method by Hydrothermal Hydrogen Reduction Technology

Guobin Zhang [1,*], Yimin Zhang [1,2,3,*], Shenxu Bao [1,3], Jing Huang [2,3] and Liuhong Zhang [3]

[1] School of Resources and Environmental Engineering, Wuhan University of Technology,
Wuhan 430070, China; soar0001@163.com

[2] School of Resources and Environmental Engineering, Wuhan University of Science and Technology,
Wuhan 430081, China; crystal208@126.com

[3] Hubei Collaborative Innovation Center for High Efficient Utilization of Vanadium Resources,
Wuhan 430081, China; zhangliuhong1994@163.com

* Correspondence: mecgbzhang@126.com (G.Z.); zym126135@126.com (Y.Z.); Tel.: +86-027-6886-2876 (Y.Z.)

Abstract: In view of the serious pollution problems caused by the traditional vanadium precipitation process, the eco-friendly technology of hydrothermal hydrogen reduction was first applied to precipitate phase pure vanadium sesquioxide (V_2O_3) products from stripped pentavalent vanadium (V (V)) solution extracted from vanadium-bearing shale. Thermodynamic analysis demonstrate the method of hydrothermal hydrogen reduction is feasible for precipitating V_2O_3 from V (V) solution at a suitable pH range, and the reduction should better be carried out at a lower pH under the pH range in which V_2O_3 can exist stably. The V_2O_3 products of 99.92% in purity and a high vanadium precipitation percentage of 99.25% were achieved under a facile reaction condition of initial solution pH of 6, reaction temperature of 523 K, H_2 partial pressure of 4 MPa and reaction time of 2 h. Based on the analysis of XRD and FE-SEM with EDS for the precipitation products obtained at serial reaction times, the phase transformation mechanism was summarized to serial reductions with the phase transformation of $H_xV_yO_z^{(2z-x-5y)-} \rightarrow NaV_2O_5 \rightarrow VO_2(H_2O)_{0.5} \rightarrow VOOH \rightarrow V_2O_3$. Compared with the two-step traditional method of precipitating vanadium with ammonium salt and roast-reduction (react at above 773 K for more than 3 h) for preparing V_2O_3, this method only experiences one-step reduction under a green atmosphere of H_2 gas with a lower reaction temperature of 523 K and a shorter reaction time of 2h. Therefore, this method for vanadium precipitation is characterized by being eco-friendly, having a short process and being low-energy consumption, which has great significance for the sustainable development of vanadium industry.

Keywords: vanadium precipitation; V_2O_3; hydrogen reduction; hydrothermal; vanadium-bearing shale

1. Introduction

Vanadium is an important metal, which has been found through a variety of applications in alloys, catalysts, advanced materials, medicine, thermistors, redox flow batteries, chemical industry, etc. [1–6]. Vanadium-bearing shale is an important vanadium-bearing resource in China, which is widely distributed in many provinces of China [7]. The gross reserves of vanadium are 118 million tons in terms of V_2O_5, accounting for more than 87% of the domestic reserves of vanadium [8,9]. Therefore, vanadium extraction from vanadium-bearing shale has been attracting increasing attention recently.

At present, the most widely applied process of extracting vanadium from vanadium-bearing shale is roasting → leaching → purification and enrichment → vanadium precipitation → calcinations

[10–15]. In order to obtain a high vanadium precipitation percentage and high-purity vanadium pentoxide (V_2O_5) product, a large amount of ammonium salt is employed as a precipitant in the process of vanadium precipitation [16–19]. As a result, a large amount of waste water containing a high concentration of ammonia and ammonia gas are respectively generated in the processes of vanadium precipitation and calcination, which produce serious water pollution and air pollution. Moreover, vanadate and decavanadate obtained by the process of vanadium precipitation with ammonium salt are highly toxic to animals due to their toxicity and accumulative behavior at specific target organs and proteins [20–23]. All these environmental problems caused by the present vanadium precipitation method restrict the sustainable development of the vanadium industry. Therefore, an environmentally friendly process of vanadium precipitation needs to be developed urgently.

In recent years, the method of hydrothermal hydrogen reduction has been developed for precipitating metal powders such as Ag, Ni, Cu, etc. from their high-valence metal ion solutions or slurries [24–27]. Through using the reduction ability of the green gas of hydrogen, the method is carried out in suitable equipment under controlled conditions of pH, temperature and H_2 partial pressure to prepare powders of the desired specification [24]. This method is considered to be easy, eco-friendly, economically feasible and low energy consumption. However, this method was rarely reported in the vanadium industry. In reality, it has been proved that under a suitable pH range pentavalent vanadium (V (V)) can stably exist as ions while trivalent vanadium (V (III)) exist as vanadium trioxide (V_2O_3) precipitates with a suitable range of vanadium concentration [28]. Therefore, if hydrogen has the ability to reduce V (V) to V (III), V_2O_3 can be precipitated by controlling the pH of V (V) solution at a suitable range. Based on this thought, we attempted to introduce the method of hydrothermal hydrogen reduction to the vanadium precipitation process in order to solve the environmentally unfriendly problems caused by the current process of vanadium precipitation with ammonium salt.

In this work, the thermodynamic feasibility and the tendency of the electromotive force of the hydrothermal hydrogen reduction for precipitating V_2O_3 products were investigated through the analysis of the potential–pH diagram for V–H_2O system. The eco-friendly hydrothermal hydrogen reduction method was developed to precipitate V_2O_3 products from a stripped V (V) solution extracted from vanadium-bearing shale. A detailed study on the effect of initial pH, reaction temperature, H_2 partial pressure and reaction time to the process of preparing V_2O_3 by hydrothermal hydrogen reduction was carried out. The phase transformation mechanism during the process of vanadium precipitation was also investigated.

2. Thermodynamic Analysis

The overall reaction of V (V) (pentavalent vanadium) in solution reduced to V_2O_3 through hydrogen reduction can be described as Equation (1). As V (V) has various species in the solution with different vanadium concentration and pH [28], the general formula of $H_xV_yO_z^{(2z-x-5y)-}$ was proposed to denote the various species of V (V) in solution.

$$2\,H_xV_yO_z^{(2z-x-5y)-} + 2y\,H_2 \rightarrow y\,V_2O_3 + (2x + 7y - 2z)\,H_2O + (4z - 10y - 2x)\,OH \tag{1}$$
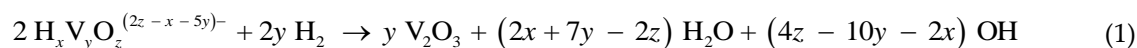
The spontaneous thermodynamic condition of the above reaction is shown in Equation (2), where ΔE is the electromotive force reflects the thermodynamic drive force of the overall reaction shown in Equation (1), $E_{H_xV_yO_z^{(2z-x-5y)-}/V_2O_3}$ is the potential of redox reaction of vanadium sesquioxide, E_{H_2O/H_2} is the potential of redox reaction of hydrogen in basic solution.

$$\Delta E = E_{H_xV_yO_z^{(2z-x-5y)-}/V_2O_3} - E_{H_2O/H_2} > 0 \tag{2}$$

To investigate the thermodynamic possibility of the reaction as shown in Equation (1), the potential–pH diagram for V–H_2O system at 298 K was developed as shown in Figure 1. To reflect the electromotive force (ΔE) of overall reaction shown in Equation (1), only the species of V (V) and V (III) were considered in this potential–pH diagram. The ΔE was also calculated and shown in Figure

1. The method of drawing this diagram was referenced to the literature [28]. As shown in Figure 1, V_2O_3 can stably exist at about pH > 2.2 and the ΔE is positive at this range of pH, which indicates that V (V) in solution can be reduced to V_2O_3 by H_2 at this range of pH in thermodynamics. It can also be seen that the ΔE value decreases as the pH of the vanadium solution increases, which indicates the hydrogen reduction (Equation (1)) tends to be more completely reactive at a lower pH under the pH range in which V_2O_3 can exist stably.
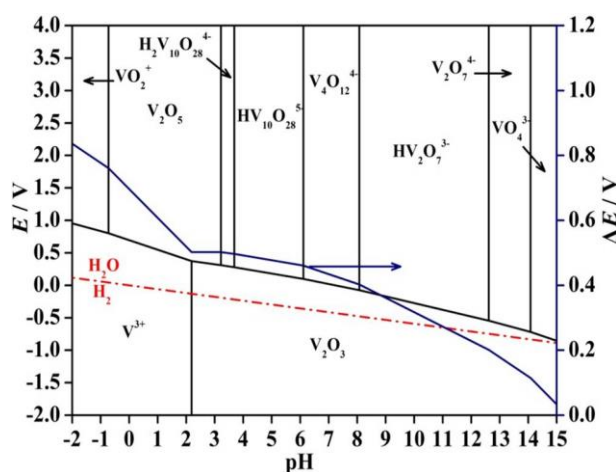
Figure 1. Potential–pH diagram for V–H_2O system (only includes V (V) and V (III) species) at 298 K with activities of dissolved vanadium of 1 mol/L and H_2 partial pressure of 1 atm.

3. Materials and Methods

3.1. Materials and Reagents

The vanadium-bearing shale was supplied by Teng-da Mining and Metallurgy Co. Ltd., Xianning, China. The ore samples were crushed and ground to less than 74 μm accounting for 70%. The chemical composition of the vanadium-bearing shale is listed in Table 1. As shown in Table 1, the content of vanadium in terms of V_2O_5 was 0.71%, indicating the raw ore is low-grade vanadium-bearing ore. The mineralogical composition of the raw ore was identified by X-ray diffraction (Figure 2). Figure 2 shows the main mineral compositions are quartz, muscovite, calcite, and pyrite. The result of electron probe micro-analysis (EPMA) of the raw vanadium-bearing shale ore is shown in Table 2. Combined Figure 2 and Table 2, it can be seen that the vanadium-bearing mineral is muscovite. Table 3 shows 71% vanadium in the raw ore exists in the form of V (III), 29% vanadium exists in the form of V (IV), and V (V) is not found in the raw ore.

The trialkylamine N235 (R_3N, R = C_8–C_{10}, tertiary amine, commercialized in China) and the tri-butyl phosphate (TBP) used in the extraction were supplied by Guoyao Chemistry Co., Ltd. (Beijing, China). H_2 gas of 99.9% in purity supplied by Wuhan Newradar Special Gas Co., Ltd. (Wuhan, China) was used as the reduction gas. N_2 gas of 99.9% in purity also supplied by Wuhan Newradar Special Gas Co., Ltd. (Wuhan, China) was used for flushing the autoclave in the experiment. $PdCl_2$ of an analytical grade supplied by Guoyao Chemistry Co., Ltd. (Beijing, China) was used as an effective catalyst. H_2SO_4 and NaOH used in this work were of analytical grade. Deionized water was employed for all tests.

Table 1. Chemical composition of vanadium-bearing shale wt %.

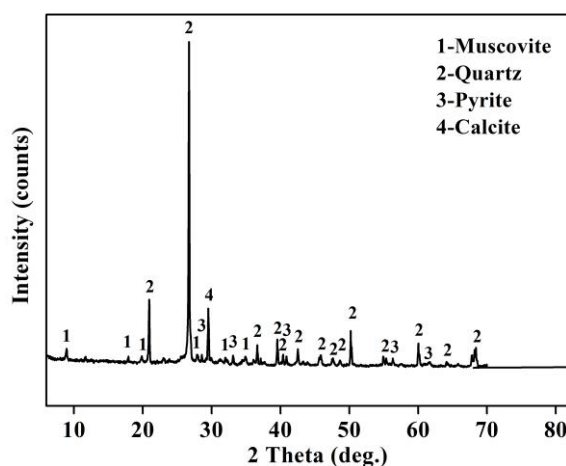| Composition	V_2O_5	Fe_2O_3	Al_2O_3	MgO	Na_2O	K_2O	CaO	SiO_2	SO_3	LOI
Content	0.71	4.99	8.91	2.18	0.38	3.02	6.26	49.28	4.35	17.82

Figure 2. XRD pattern of raw vanadium-bearing shale ore.

Table 2. EPMA result of raw vanadium-bearing shale ore wt %.

Minerals	V_2O_5	SiO_2	Al_2O_3	MgO	K_2O	CaO	FeO
Muscovite	3.52	49.09	27.31	4.49	9.56	0.02	0.18
Quartz	0	98.43	0	0	0	0	0
Pyrite	0	0.05	0	0	0	0	59.13
Calcite	0	0	0	1.10	0	65.94	0

Table 3. Vanadium valence states analysis of raw ore, blank roasted ore and leaching solution wt %.

Contents	Vanadium Valence State		
	V (III)	V (IV)	V (V)
Raw ore	71	29	0
Blank roasted ore	44	52	4
Leaching solution	0	0	100

3.2. Procedures and Characterizations

3.2.1. Preparation of Stripped V (V) Solution

The process flow sheet for preparing the stripped V (V) solution from the vanadium-bearing shale is proposed in Figure 3 [29]. First, the vanadium-bearing shale was roasted at 1123 K for 1 h in air. As shown in Table 3, after roasting, V (IV) in the sample increased from 28% to 52%, V (V) increased from 0% to 4%, whereas V (III) decreased from 77% to 44%. The results reveal low valance vanadium (V (III) and V (IV)) has been partially converted to high valence vanadium (V (IV) or V (V)) which are more easily to be leached out by sulfuric acid. Then, by leaching the blank roasted ore (blank roasted vanadium-bearing shale ore) with 15% (*v/v*) H_2SO_4 and 0.8% (wt) $NaClO_3$ (used as oxidant) at 368 K and liquid/solid ratio of 1.5 for 6 h, followed by solid-liquid separation, the leaching solution was obtained. Table 3 shows the vanadium in the leaching solution totally exists in the form of V (V). Afterwards, using 400 g/L NaOH solution to adjust the pH of the leaching solution to about 1.6, followed by three stages of extraction under the following condition: organic solution consist of 20% (*v/v*) trialkylamine (N235) and 5% (*v/v*) tri-butyl phosphate (TBP), A/O phase ratio of 3 and equilibrium time of 5 min, the loaded organic phase was prepared. After that, the loaded organic phase was scrubbed by 0.5 mol/L H_2SO_4 solution for three stages at an O/A radio of 1, and then was washed to pH above 4 by deionized water. At last, using 1 mol/L NaOH solution to strip the scrubbed loaded organic phase for four stages under a condition of O/A radio of 6 and equilibrium time of 6 min, a colorless stripped V (V) solution with pH value of about 13 and vanadium concentrate of 20.23 g/L was obtained. The main chemical composition of the stripped V (V) solution is listed in Table 4. The results show that the main ions in the stripped V (V) solution are V and Na, impurity ions which

may be harmful to the vanadium precipitation have been effectively removed through the process shown in Figure 3.
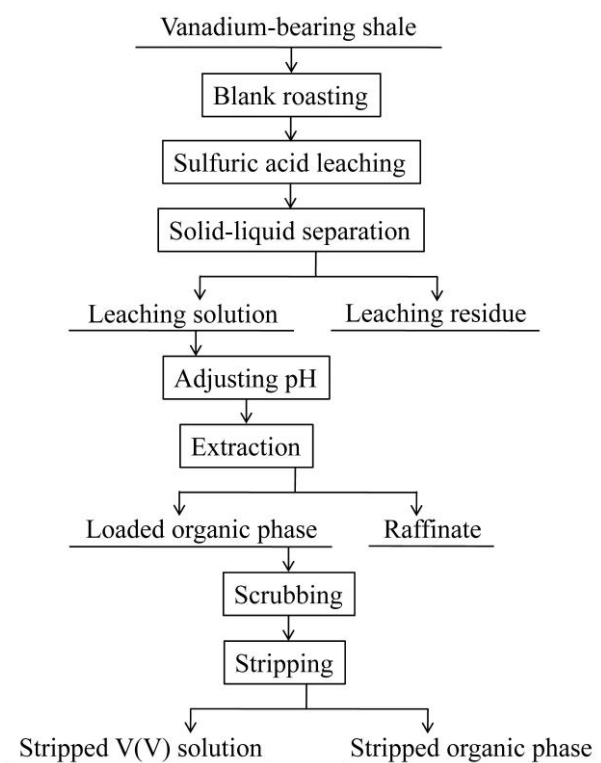
Figure 3. Proposed process flow sheet for preparation of stripped V (V) solution from vanadium-bearing shale.

Table 4. Main chemical composition of the stripped V (V) solution.

Items	V	Fe	Al	Mg	Na	K	Ca	P	Si
Concentration (g/L)	20.32	0.009	0.014	0.008	23.05	0	0	0.021	0.013

3.2.2. Vanadium Precipitation of Hydrothermal Hydrogen Reduction

The process of vanadium precipitation of hydrothermal hydrogen reduction is performed as follows. First, 50% (*v/v*) sulfuric acid solution was used to adjust the pH of the 500mL stripped V (V) solution to a certain value, and then the feed solution was obtained. Secondly the feed solution and 10 mg $PdCl_2$ were transferred into a 1000 mL autoclave. Herein, $PdCl_2$ acts as an effective catalyst in the hydrothermal hydrogen reduction process because it is easily reduced to metallic Pd by hydrogen which can absorb 700 times volume of hydrogen gas and turn the adsorbed hydrogen to active hydrogen (H*) for reduction reaction [27]. After being flushed a few times with N_2 gas, the autoclave started to be heated. Once the reaction temperature reached to the predetermined temperature the hydrogen gas with a certain partial pressure was introduced into the autoclave. After maintaining the reaction at the predetermined temperature and stirring rate of 800 rpm for different time durations, the autoclave was cooled to room temperature. At last the precipitate was collected by filtration, washed with deionized water for several times and dried at 353 K in a vacuum drying oven to obtain the vanadium-bearing products.

3.2.3. Characterizations

The chemical composition of the vanadium-bearing shale, the stripped V (V) solution and the obtained vanadium-bearing products were analyzed by inductively coupled plasma–optical emission spectroscopy (ICP–OES, Optima 4300DV, Perkin–Elmer, Waltham, MA, USA). The crystal structure of the raw ore and the products were obtained by a D/MAX-RB X-ray diffractometer (Rigaku, Tokyo, Japan), using Cu Kα radiation (λ = 0.15406 nm) at 40 KV and 40 KA. A JAX-8230 electron probe micro-analyzer (EPMA, JEOL Ltd., Tokyo, Japan) was applied for quantitative elementary analysis and mineralogical composition. The vanadium valence states of the raw ore, blank roasted ore and the leaching solution were measured on an automatic potentiometric titrimeter (model ZDJ-4A) using the ammonium ferrous sulfate method. The morphologies and the microchemical-analysis of synthesized powders were characterized by field emission scanning electron microscopy (FE-SEM, Zeiss Ultra Plus, Carl Zeiss AG, Oberkochen, Germany) with X-ray energy dispersive spectroscopy (EDS, X-MAX 50, Oxford Instruments, Oxford, UK).

3.3. Data Treatment

The vanadium precipitation percentage (%P) was calculated based on Equation (3). In the equation C_M and C_F represent the concentrations of vanadium in the vanadium precipitated liquor and feed solution, respectively. V_M and V_F represent the volume of the vanadium precipitated liquor and feed solution, respectively.

$$\%\,P = (1\,-\,C_M V_M / C_F V_F) \times 100 \tag{3}$$

4. Results and Discussion

4.1. Effect of Initial Solution pH on Vanadium Precipitation

The effects of initial solution pH on the vanadium precipitation percentage and the phase of the precipitates were studied under the following conditions; reaction temperature of 523 K, reaction time of 8 h, H_2 partial pressure of 4 MPa. The results are presented in Figure 4.
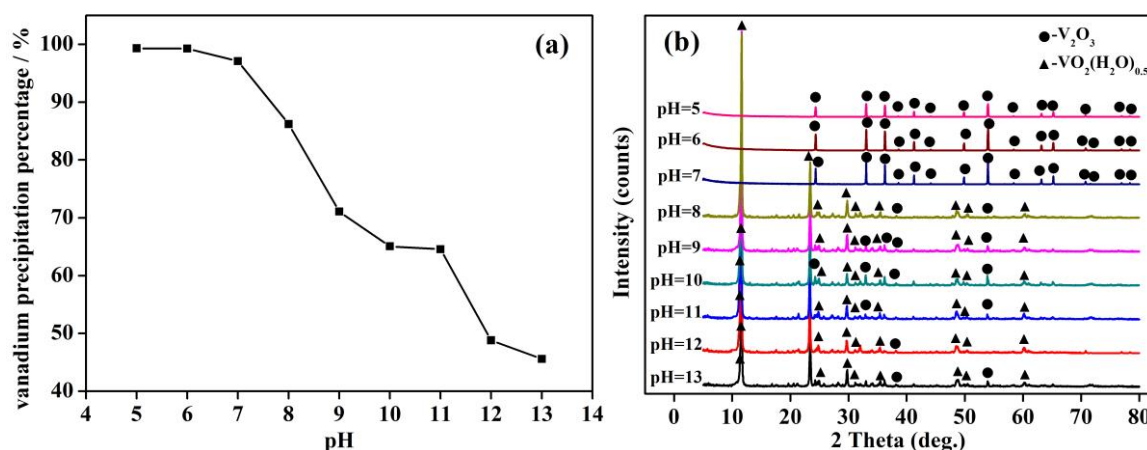

Figure 4. (**a**) Effect of initial solution pH on the vanadium precipitation percentage; (**b**) XRD patterns of the precipitates obtained at different initial solution pH.

Figure 4 shows the initial solution pH has significant effects both on vanadium precipitation percentage and the phase of the precipitates. As shown in Figure 4a, the vanadium precipitation percentage decreases from 99.33% to 45.60% as the initial solution pH increases from 5 to 13. The XRD patterns of the precipitates presented in Figure 4b show that the diffraction peaks can be indexed to a single phase of V_2O_3 when the pH ranging from 5 to 7, whereas the diffraction peaks are indexed to a mixture phase of $VO_2(H_2O)_{0.5}$ and V_2O_3 when the initial solution pH ranging from 8 to 13. The results

indicate that the complete degree of the reaction decreases with the increases of the initial solution pH value.

To better investigate the reduction of V (V) in solution to V_2O_3, the potential–pH diagram for V–H_2O system (includes all the vanadium species whose thermodynamic data can be indexed) at 298 K was developed as shown in Figure 5. It can be revealed from Figure 5 that V_2O_3 is the final products of the reduction. It is considered to be feasible that if the thermodynamic drive force or the hydrogen activity is not enough the reduction will not be complete and the V (IV) species (shown in Figure 5) will be appeared in the products. It has been discussed in Figure 1 that the increase of the pH of the vanadium solution results in the decrease of the ΔE value which reflects the decrease of the thermodynamic drive force of the reduction. Combined with the results shown in Figure 4, it can be inferred that the thermodynamic drive force is enough for the reduction of V (V) to V_2O_3 under the pH range of 5 to 7, however, with the pH of the solution increases above 8 the thermodynamic drive force is unable to make the reduction complete which result in the products as mixture phases of V_2O_3 and a V (IV) species of $VO_2(H_2O)_{0.5}$. Herein, we infer that the V (IV) species in the products is not VO_2 shown in Figure 5 but $VO_2(H_2O)_{0.5}$ maybe due to the hydrothermal reaction condition.
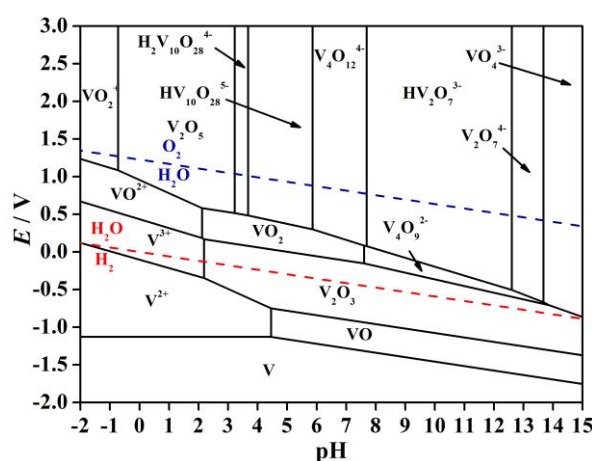

Figure 5. Potential–pH diagram for V–H_2O system at 298 K with activities of dissolved vanadium of 1 mol/L and H_2 partial pressure of 1 atm.

Based on the above analysis, the initial solution pH should better be kept below 7 in order to obtain high purity V_2O_3 products. Concerning that the vanadium precipitation percentage was no longer decreased from the initial solution pH of 5 to 6 shown in Figure 4a and to economize the consumption of sulfuric acid in adjusting the solution pH, the suitable initial solution pH was selected as 6.

4.2 Effect of Reaction Time on Vanadium Precipitation

The effect of reaction time on the vanadium precipitation percentage and the phase of the precipitates were studied under the following conditions; reaction temperature of 523 K, initial solution pH of 6, H_2 partial pressure of 4 MPa. The results are presented in Figure 6. Figure 6a shows the vanadium precipitation percentage increases to 99.25% at 2 h, and no further obvious increase can be observed after this, which indicates almost all vanadium in the solution can be precipitated within 2 h. The XRD patterns presented in Figure 6b show that the diffraction peaks of the powders obtained at 1 h are indexed to a mixture phase of $VO_2(H_2O)_{0.5}$, VOOH and V_2O_3, after reaction for 2h all the diffraction peaks of the obtained powders are indexed to a single phase of V_2O_3. This result demonstrates the precipitates can be totally transformed to the final products of V_2O_3 within 2 h. Therefore, the results reveal that the reduction can be fully carried out within 2 h. In consideration of saving energy consumption, the suitable reaction time was selected as 2 h.
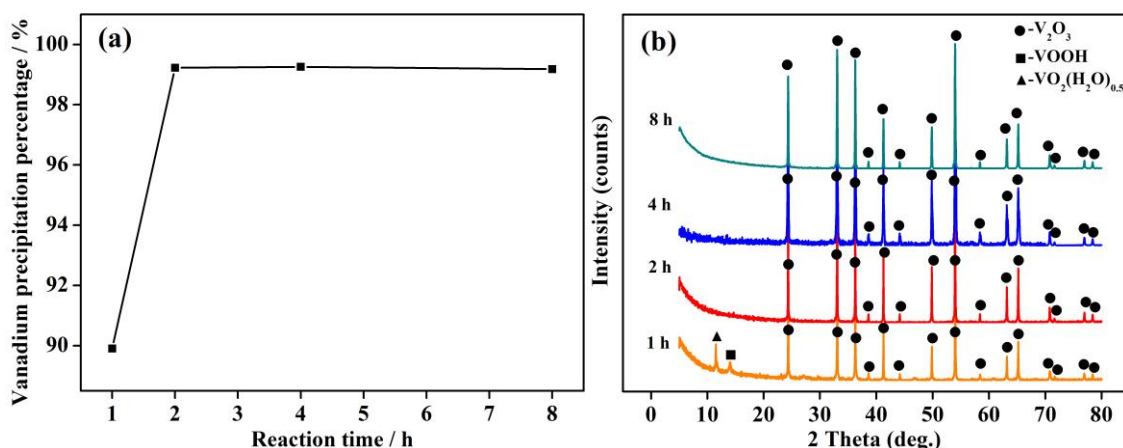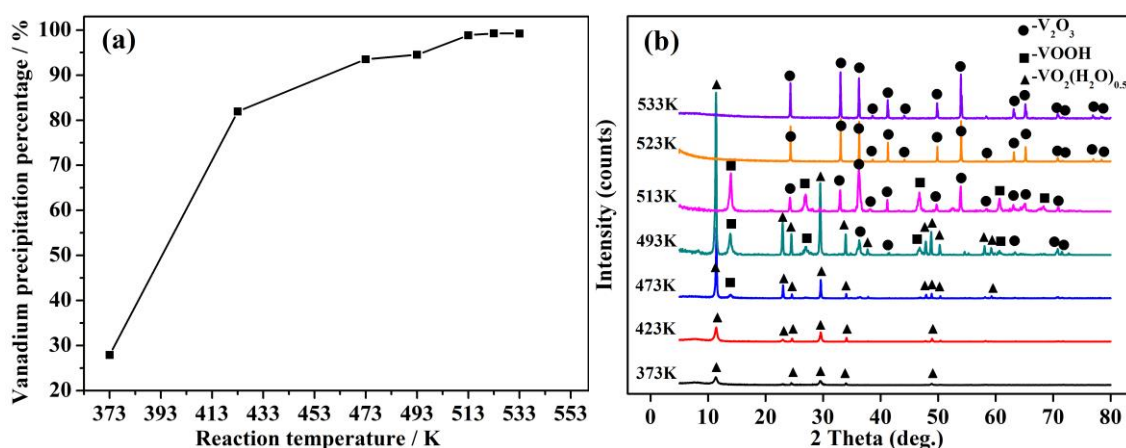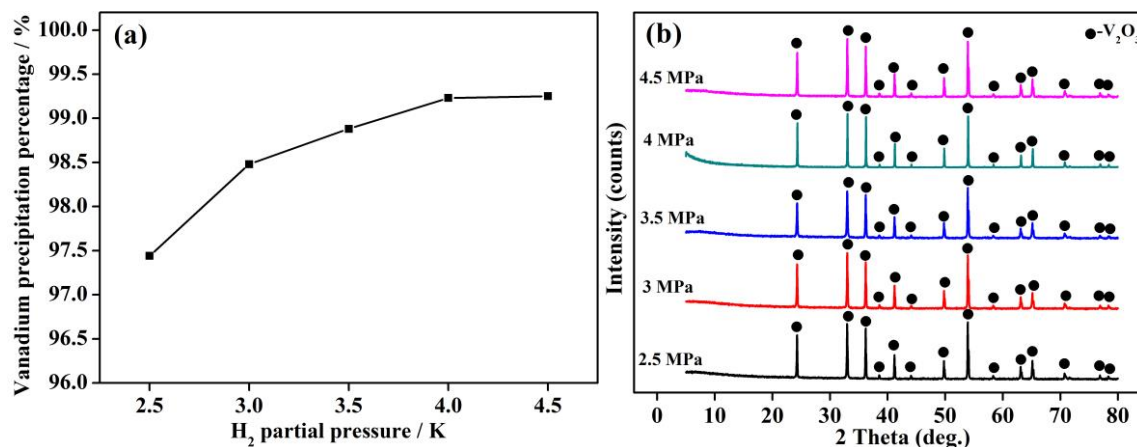
Figure 6. (**a**) Effect of reaction time on the vanadium precipitation percentage; (**b**) XRD patterns of the precipitates obtained at different reaction time.

4.3. Effect of Reaction Temperature on Vanadium Precipitation

The effect of reaction temperature on the vanadium precipitation percentage and the phase of the precipitates were studied under the following conditions; initial solution pH of 6, reaction time of 2 h, H_2 partial pressure of 4 MPa. The results are presented in Figure 7.

Figure 7. (**a**) Effect of reaction temperature on the vanadium precipitation percentage; (**b**) XRD patterns of the precipitates obtained at different reaction temperature.

Figure 7 shows the reaction temperature also has significant effects both on vanadium precipitation percentage and the phase of the precipitates. Figure 7a shows the vanadium precipitation percentage increases from 27.91% to 99.25% as the reaction temperature increases from 373 K to 523 K, and no future obvious increase is observed after reacting for 523 K. The XRD patterns presented in Figure 7b show that the diffraction peaks of the powders obtained at 373 K and 423 K are all indexed to the phase of $VO_2(H_2O)_{0.5}$, as the reaction temperature reach to 473 K the diffraction peaks refer to the phase of VOOH appear in the XRD pattern of the obtained powders, the diffraction peaks refer to the phase of V_2O_3 can be observed in the XRD patterns of the obtained powders when the reaction temperature is above 493 K, the pure phase of V_2O_3 appear as the reaction time reach to 523 K. This result demonstrates the phase pure V_2O_3 products need to be obtained at a temperature no lower than 523 K. Moreover, the results indicate that the complete degree of the reaction increases with the increase of the reaction temperature. This may be because the activity of the hydrogen increases with the reaction temperature increases, which cause the increase of the thermodynamic drive force for the reaction. Therefore, raising the temperature is conducive to the reaction, in consideration of saving energy consumption the suitable reaction temperature was selected as 523 K.

4.4. H$_2$ partial Pressureon Vanadium Precipitation

The effect of H$_2$ partial pressure on the vanadium precipitation percentage and the phase of the precipitates were studied under the following conditions; reaction temperature of 523 K, initial solution pH of 6, reaction time of 2 h. Herein, the selected H$_2$ partial pressures can ensure the amount of hydrogen needed for the reaction of reducing V (V) to V (III). The results are presented in Figure 8.

Figure 8. (**a**) Effect of H$_2$ partial pressure on the vanadium precipitation percentage; (**b**) XRD patterns of the precipitates obtained at different H$_2$ partial pressure.

Figure 8a shows the vanadium precipitation percentage increases from 97.44% to 99.25% as the H$_2$ partial pressure increases from 2.5 MPa to 4.0 MPa, no further obvious increase is observed after this. The XRD patterns presented in Figure 8b show that the diffraction peaks of the powders obtained at 2.5 MPa, 3 MPa, 4 MPa and 4.5 MPa are all indexed to the phase of V$_2$O$_3$, which indicate the H$_2$ partial pressure has no obvious effect to the phase of the precipitate when the H$_2$ partial pressure can ensure the amount of hydrogen needed for the reaction of reducing V (V) to V (III). Concerning about the recovery of the vanadium the suitable H$_2$ partial pressure was selected as 4.0 MPa.

Based on the above singe-factor experiments, it is feasible to precipitate V$_2$O$_3$ product from stripped V (V) solution extracted from vanadium-bearing shale with a high vanadium precipitation percentage of 99.25% via the method of hydrothermal hydrogen reduction under a facile condition of initial solution pH of 6, reaction temperature of 523 K, H$_2$ partial pressure of 4 MPa and reaction time of 2 h. The chemical composition of the V$_2$O$_3$ product obtained under the above optimal conditions is shown in Table 5. The purity of the V$_2$O$_3$ product can reach 99.92%, and the impurities are in trace amounts.

Table 5. Chemical composition of V$_2$O$_3$ products obtained at 523 K for 2 h with H$_2$ partial pressure of 4 MPa and reaction time of 2 h wt %.

Composition	V$_2$O$_3$	Fe	Si	P	S	K$_2$O	Na$_2$O	As
Content	99.92	0.001	0.003	0.008	0.002	0	0.03	0

We highlight that this method for vanadium precipitation is eco-friendly compared with the traditional process of precipitate vanadium with ammonium salt because the H$_2$ gas used in the vanadium precipitation is a green gas which is no harmful to the environment. Moreover, the products obtained by the traditional vanadium precipitation belong to ammonium vanadates which need to be calcined above 773 K under a suitable reductive atmosphere to prepare V$_2$O$_3$. However, the calcining process can be omitted for preparing V$_2$O$_3$ by using the method of hydrothermal hydrogen reduction. Therefore, the method also has the advantages of short process and low energy consumption from the perspective of preparation of vanadium sesquioxide.

4.5. Phase Transformation Mechanismof the Vanadium Precipitation

To investigate the phase transformation mechanism during the process of vanadium precipitation, serial experiments with various heating time were conducted. Reduction products obtained under the following conditions of reaction temperature of 523 K, initial solution pH of 6 and H_2 partial pressure of 4 MPa for 0.5 h, 1 h and 2 h were taken as representatives for demonstrating the typical transformation stages.

The XRD patterns of the precipitates obtained at different heating time are shown in Figure 9, describing the structural transformation processes of the products. As shown in Figure 9a, a mixture phase of NaV_2O_5 and $VO_2(H_2O)_{0.5}$ can be observed after the reaction last for 0.5 h. Increasing the reaction time to 1 h the phase of NaV_2O_5 disappears and the diffraction peaks refer to $VO_2(H_2O)_{0.5}$ decrease in intensity with the appearance of the phase of VOOH and V_2O_3 as shown in Figure 9b. Figure 9c shows the mixture phase totally transforms into a single phase of V_2O_3 after the reaction last for 2 h.
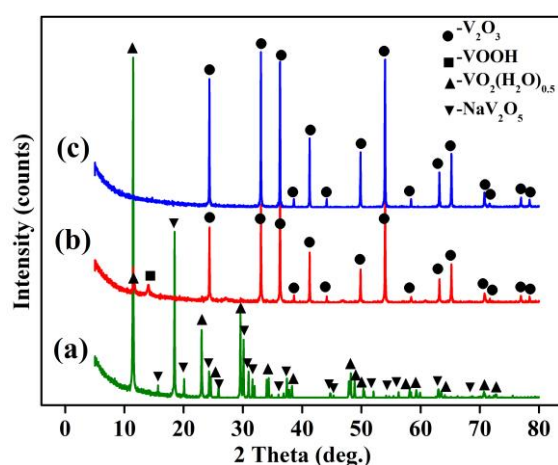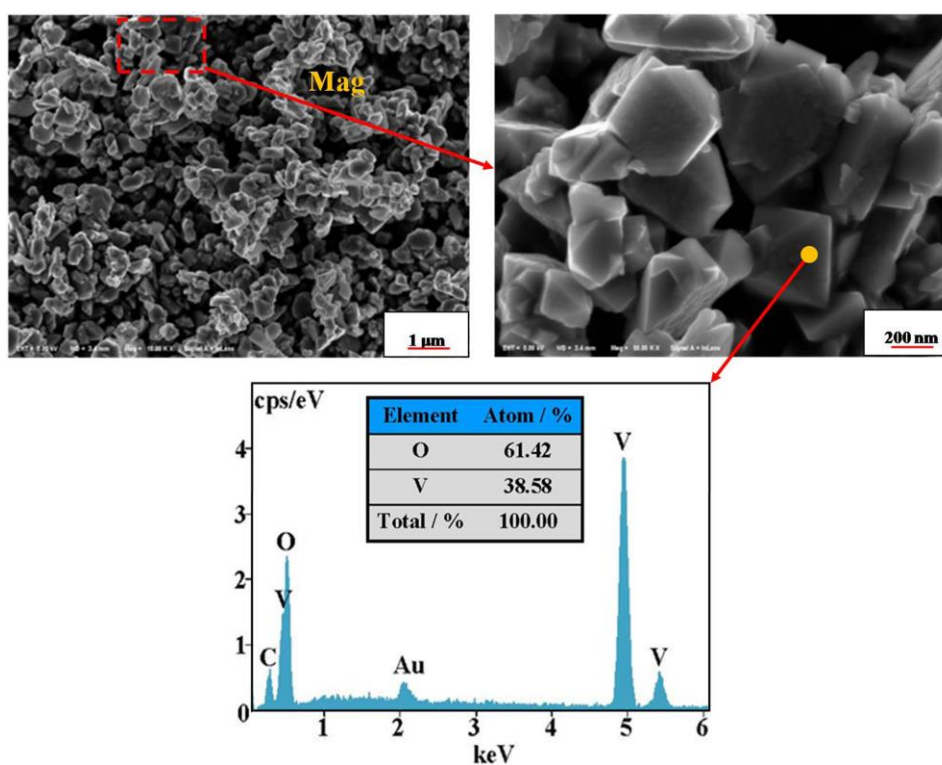

Figure 9. XRD patterns of the powders obtained at (**a**) 0.5 h, (**b**) 1 h and (**c**) 2 h.

Figure 10 demonstrates the typical field emission scanning electron microscope (FE-SEM) images with the analysis of the X-ray energy dispersive spectroscopy (EDS) which can intuitively illustrate the morphology and the phase change with increasing reaction time during the process of vanadium precipitation. When the reaction last for 0.5 h, the products are composed of clubs and sheets which can be identified as NaV_2O_5 and $VO_2(H_2O)_{0.5}$ respectively according to the analysis of the EDS (Figure 10a). When the reaction time increases to 1 h, the clubs disappear and the reaction products are almost entirely composed of granules which can be ascertained as V_2O_3 according to the analysis of the EDS (Figure 10b). When the reaction last for 2 h, the reaction products are all composed of granules which can be identified as V_2O_3 according to the analysis of the EDS (Figure 10c). The results of the EDS consist well with the analysis of the XRD patterns shown in Figure 9. It also can be seen from the FE-SEM images (Figure 10c) the as obtained V_2O_3 products demonstrate orthorhombic structure and some particles display the tetragonal dipyramids shape.

Based on the results of XRD (Figure 9) and FE-SEM with EDS (Figure 10) respectively, the evolution in structure and morphology by changing the reaction time can be used to investigate the phase transformation process during the vanadium precipitation. Figure 11 shows that the pH of the reaction solution increases gradually during the reduction process through measuring the pH of the filtered solution after reacting for different times. Hence, the main chemical reactions involved in the vanadium precipitation via the method of hydrothermal hydrogen reduction are proposed as Equations (4)–(10).
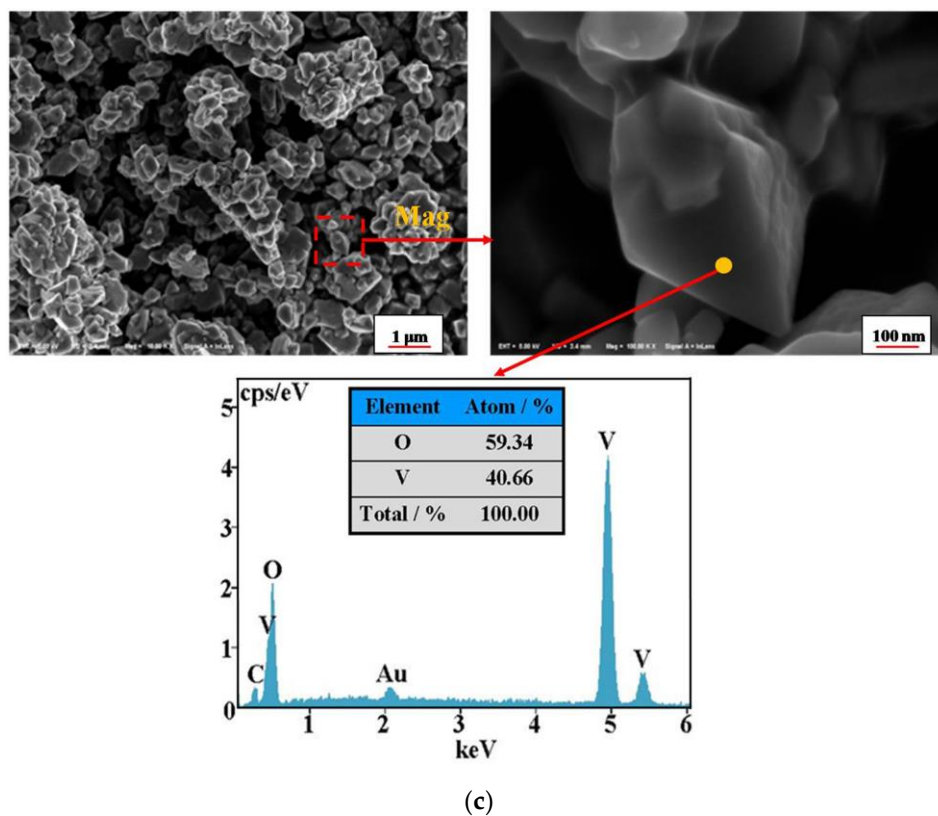
(**a**)

(**b**)

(**c**)
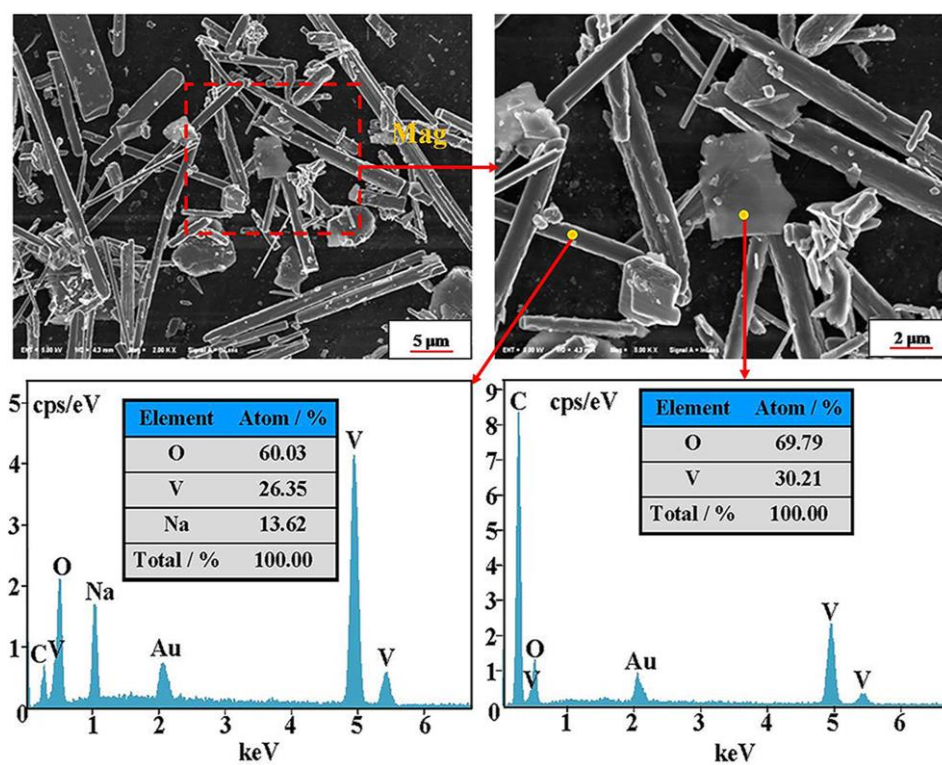
Figure 10. FE-SEM images with EDS analysis of the powders obtained at (**a**) 0.5 h, (**b**) 1 h and (**c**) 2 h.
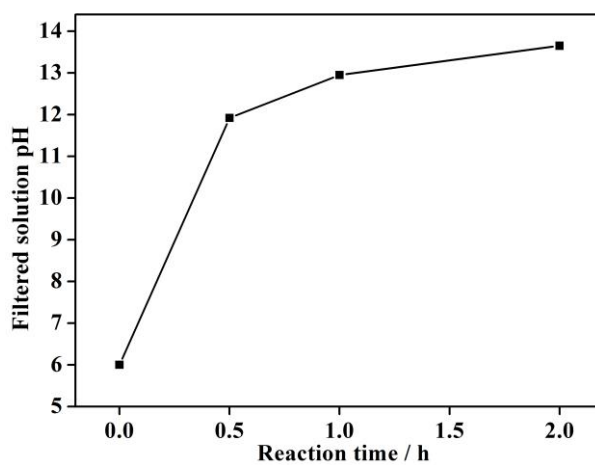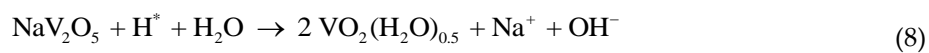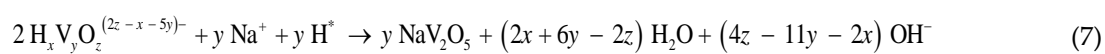

Figure 11. Effect of reaction time on the pH of filtered solution.

$$H_2(g) \rightleftarrows H_2(l) \tag{4}$$

$$PdCl_2 + H_2(l) \rightarrow Pd + 2H^+ + 2Cl^- \tag{5}$$

$$Pd + H_2(l) \rightarrow Pd + 2H^* \tag{6}$$

$$2H_xV_yO_z^{(2z-x-5y)-} + yNa^+ + yH^* \rightarrow yNaV_2O_5 + (2x+6y-2z)H_2O + (4z-11y-2x)OH^- \tag{7}$$

$$NaV_2O_5 + H^* + H_2O \rightarrow 2VO_2(H_2O)_{0.5} + Na^+ + OH^- \tag{8}$$

$$2VO_2(H_2O)_{0.5} + 2H^* \rightarrow 2VOOH + H_2O \tag{9}$$

$$2\,VOOH + 2\,H^* \rightarrow V_2O_3 + H_2O \tag{10}$$
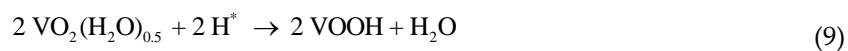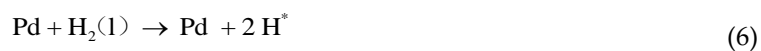
　　Equations (4)–(6) reveal the process of the H_2 activated to the active hydrogen (H*) by the $PdCl_2$. H_2 (g) (hydrogen gas) firstly dissolved into the V (V) solution, then the catalyst $PdCl_2$ is reduced to metallic Pd by those dissolved hydrogen, afterwards, the metallic Pd absorb the dissolved hydrogen and turn the absorbed hydrogen into H* (active hydrogen) [27]. Equations (7)–(10) reveal the process of V (V) in the stripped solution transformed to the V_2O_3 precipitates. V (V) in the stripped solution should be first reduced to $V_2O_5^-$ by the H*. Due to the existence of Na^+, the club-shaped NaV_2O_5 precipitates are crystallized out from the solution when the concentration of NaV_2O_5 is higher than its saturation solubility under a suitable pH range. The V whose average valence is +4.5 in the NaV_2O_5 precipitates and $V_2O_5^-$ is further reduced to the V (IV) and crystallized in the form of sheet-like $VO_2(H_2O)_{0.5}$ precipitates. At the same time, Na^+ dissolves in the solution, which make the final product is no polluted by this ion. After that, the $VO_2(H_2O)_{0.5}$ is reduced and hydrolyzed to the VOOH. Finally, the VOOH dehydrate with each other and transform to the orthorhombic V_2O_3. XRD patterns in Figure 9 clearly illustrate the reaction process of Equations (7)–(10). Thus, the phase transformation mechanism of the vanadium precipitation can be describe as serial reductions with the phase transformation of $H_xV_yO_z^{(2z-x-5y)-} \rightarrow NaV_2O_5 \rightarrow VO_2(H_2O)_{0.5} \rightarrow VOOH \rightarrow V_2O_3$.

5. Conclusions

(1)　According to the thermodynamic analysis, it is feasible for V (V) in solution to be reduced to V (III) in forms of V_2O_3 by H_2 gas under a suitable range of solution pH value. In addition, the electromotive force (ΔE) reflects the thermodynamic drive force of the overall reduction decreases as the pH value of the vanadium solution increases, which indicates the hydrogen reduction tends to be more completely reactive at a lower pH value under the pH range in which V_2O_3 can exist stably.

(2)　The V_2O_3 products of 99.85% in purity were precipitated from stripped V (V) solution extracted from vanadium-bearing shale with a high vanadium precipitation percentage of 99.25% via the method of hydrothermal hydrogen reduction under a facile condition of initial solution pH of 6, reaction temperature of 523 K, H_2 partial pressure of 4 MPa and reaction time of 2 h.

(3)　The phase transformation mechanism of the vanadium precipitation process proposed in this paper can be described as follows. In the reduction of activated hydrogen, V (V) in solution is first reduced to $V_2O_5^-$ in forms of NaV_2O_5 with Na^+, then NaV_2O_5 is reduced to V (IV) in forms of $VO_2(H_2O)_{0.5}$ which is further reduced and hydrolyzed to the VOOH, at last the VOOH dehydrate with each other and transform to the orthorhombic V_2O_3. This process can be summarized as serial reductions with the phase transformation of $H_xV_yO_z^{(2z-x-5y)-} \rightarrow NaV_2O_5 \rightarrow VO_2(H_2O)_{0.5} \rightarrow VOOH \rightarrow V_2O_3$.

　　In summary, the technology of hydrothermal hydrogen reduction was first successfully developed as a vanadium precipitation method to precipitated phase pure V_2O_3 products. Compared with the two-step traditional method of precipitating vanadium with ammonium salt and roast-reduction (react at above 773 K for more than 3 h) for preparing V_2O_3, this method only experiences one-step reduction under a green atmosphere of H_2 gas with a lower reaction temperature of 523 K and a shorter reaction time of 2h. Therefore, the method is characterized by being eco-friendly, short-process and having low-energy consumption, which has great significance for the sustainable development of vanadium industry.

Author Contributions: Guobin Zhang and Yimin Zhang provided the original ideas and designed the experiments; Guobin Zhang and Liuhong Zhang performed the experiments; Guobin Zhang analyzed the data; Shenxu Bao and Jing Huang contributed reagents/materials/analysis tools; Guobin Zhang wrote the paper.

Conflicts of Interest: The authors declare no conflict of interest.

References

1. Moskalyk, R.R.; Alfantazi, A.M. Processing of vanadium: A review. *Miner. Eng.* **2003**, *16*, 793–805.
2. Zhang, G.; Chen, D.; Zhao,W.; Zhao, H.; Wang, L.; Li, D.; Qi, T. A novel synergistic extraction method for recovering vanadium (V) from high-acidity chloride leaching liquor. *Sep. Purif. Technol.* **2016**, *165*, 166–172.
3. Yang, X.; Zhang, Y.; Bao, S. Preparation high purity V_2O_5 from a typical low-grade refractory stone coal using a pyro-hydrometallurgical process. *Minerals* **2016**, *6*, 69.
4. Chen, F.; Zhang, Y.; Huang, J.; Liu, T.; Xue, N. Mechanism of enhancing extraction of vanadium from stone coal by roasting with MgO. *Minerals* **2017**, *7*, 33.
5. Skyllaskazacos, M.; Cao, L.Y.; Kazacos, M.; Kausar, N.; Mousa, A. Vanadium electrolyte studies for the vanadium redox battery—A review. *Cheminform* **2016**, *47*, 1521–1543.
6. Zheng, Q.; Zhang, Y.; Huang, J.; Liu, T.; Xue, N.; Shi, Q. Optimal location of vanadium in muscovite and its geometrical and electronic properties by DFT calculation. *Minerals* **2017**, *7*, 32.
7. Zhang, Y.; Bao, S.; Liu, T.; Chen, T.; Huang, J. The technology of extracting vanadium from stone coal in China: History, current status and future prospects. *Hydrometallurgy* **2011**, *109*, 116–124.
8. Hu, P.; Zhang, Y.; Liu, T.; Huang, J.; Yuan, Y. Highly selective separation of vanadium over iron from stone coal by oxalic acid leaching. *Ind. Eng. Chem.* **2017**, *45*, 241–247.
9. Wang, B.; Liu, T.; Zhang, Y.; Huang, J. Effect of CaF_2/CaO composite additive on roasting of vanadium-bearing stone coal and acid leaching kinetics. *Minerals* **2017**, *7*, 43.
10. Cai, Z.; Zhang, Y.; Liu, T.; Huang, J. Mechanisms of vanadium recovery from stone coal by novel $BaCO_3$/CaO composite additive roasting. *Minerals* **2016**, *6*, 26.
11. Liu, Y.; Yang, C.; Li, P.; Li, S. A new process of extracting vanadium from stone coal. *Int. J. Miner. Metall. Mater.* **2010**, *17*, 381–388.
12. Li, X.; Xie, B. Extraction of vanadium from high calcium vanadium slag using direct roasting and soda leaching. *Int. J. Miner. Metall. Mater.***2012**, *19*, 595–601.
13. He, D.; Feng, Q.; Zhang, G.; Ou, L.; Lu, Y. An environmentally-friendly technology of vanadium extraction from stone coal. *Miner. Eng.* **2007**, *2011*, 84–1186.
14. Wang, M.; Xiao, L.; Li, Q.; Wang, X.; Xiang, X. Leaching of vanadium from stone coal with sulfuric acid. *Rare Metals* **2009**, *28*, 1–4.
15. Chen, X.; Lan, X.; Zhang, Q.; Ma, H.; Zhou, J. Leaching vanadium by high concentration sulfuric acid from stone coal. *Trans. Non-Ferrous Metall. Soc. China* **2010**, *20*, s123–s126.
16. Deng, Z.; Wei, C.; Fan, G.; Li, M.; Li, C.; Li, X. Extracting vanadium from stone-coal by oxygen pressure acid leaching and solvent extraction. *Trans. Non-Ferrous Metall. Soc. China* **2010**, *20*, s118–s122.
17. Wang, X.; Wang, M.; Shi, L.; Hu, J.; Qiao, P. Recovery of vanadium during ammonium molybdate production using ion exchange. *Hydrometallurgy* **2010**, *104*, 317–321.
18. Ning, P.; Lin, X.;Wang, X.; Cao, H. High-efficient extraction of vanadium and its application in the utilization of the chromium-bearing vanadium slag. *Chem. Eng. J.* **2016**, *301*, 132–138.
19. Wang, Y.; Li, D.; Zhang, H. Main factors affecting precipitation of vanadium with acidic ammonium salt and its countermeasures. *Iron Alloy***2012**, *4*, 12–16. (In Chinese)
20. Soares, S.S.; Gutiérrez-Merino, C.; Aureliano, M. Mitochondria as a target for decavanadate toxicity in sparus aurata heart. *Aquat. Toxicol.* **2007**, *83*, 1–9.
21. Aureliano, M. Decavanadate toxicology and pharmacological activities: V10 or V1, both or nandone? *Oxid. Med. Cell. Longev.* **2016**, *2016*, 1–8.
22. Fraqueza, G.; Ohlin, A.C.; Casey, W.H.; Aureliano, M. Sarcoplasmic reticulum calcium ATPase interactions with decaniobate, decavanadate, vanadate, tungstate and molybdate. *J. Inorg. Biochem.* **2012**, *107*, 82–89.
23. Aureliano, M.; Ohlin, A.C. Decavanadate in vitro and in vivo effects: Facts and opinions. *J. Inorg. Biochem.* **2014**, *137*, 123–130.
24. Agrawal, A.; Kumar, V.; Pandey, B.D.; Sahu, K.K. A comprehensive review on the hydro metallurgical process for the production of nickel and copper powders by hydrogen reduction. *Mater. Res. Bull.* **2006**, *41*, 879–892.
25. Yu, K.; Liang, H. Attempt at preparing Cu by direct hydrogen reduction of Cu_2S slurry. *Mater. Lett.* **2004**, *58*, 3045–3048.
26. Saarinen, T.; Lindfors, L.E.; Fugleberg, S. A review of the precipitation of nickel from salt solutions by hydrogen reduction. *Hydrometallurgy* **1998**, *47*, 309–324.

27. Liang, H.; Tang, Q.; Yu, K.; Li, S.; Ke, J. Preparation of metallic silver from Ag₂S slurry by direct hydrogen reduction under hydrothermal conditions. *Mater. Lett.* **2007**, *61*, 1020–1022.

28. Zhou, X.; Wei, C.; Li, M.; Qiu, S.; Li, X. Thermodynamics of vanadium-sulfur-water systems at 298 K. *Hydrometallurgy* **2011**, *106*, 104–112.

29. Yang, X.; Zhang, Y.; Bao, S.; Shen, C. Separation and recovery of vanadium from a sulfuric-acid leaching solution of stone coal by solvent extraction using trialkylamine. *Sep. Purif. Technol.* **2016**, *164*, 49–55.